

---

# Optical properties of organic haze analogues in water-rich exoplanet atmospheres observable with JWST

---

In the format provided by the authors and unedited

---

## **Table of Contents**

Supplementary Table 1.....	2
Supplementary Table 2.....	3
Supplementary Table 3.....	5
Supplementary Figure 1.....	6
Supplementary Figure 2.....	7
Supplementary Figure 3.....	8
Supplementary Figure 4.....	9
Supplementary Figure 5.....	10
Supplementary Figure 6.....	11

**Supplementary Table 1.** The density and elemental compositions of the two haze analogues in this study with their initial gas compositions. The results for PHAZER produced Titan, Triton, and Pluto haze analogues are listed for comparison.<sup>18,31</sup>

	Particle density (g cm <sup>-3</sup> )	Elemental compositions	Initial gases
400 K (Exoplanet)	1.262	C: 56%±2.5% H: 6.1%±0.2% N: 21.1%±0.5% O: 17%±3.2%	56% H <sub>2</sub> O 11% CH <sub>4</sub> 10% CO <sub>2</sub> 6.4% N <sub>2</sub> 1.9% H <sub>2</sub> 14.7% He
300 K (Exoplanet)	1.328	C: 51%±1.2% H: 6.1%±0.1% N: 27.1%±0.7% O: 15%±2.0%	66% H <sub>2</sub> O 6.6% CH <sub>4</sub> 6.5% N <sub>2</sub> 4.9% CO <sub>2</sub> 16% He
100 K (Titan/Triton/Pluto)	1.343-1.424	C: 49.6-46.2%* H: 5.6-5.3%* N: 42.5-39.8%* O: 2.2-8.6%*	95-90% N <sub>2</sub> 5% CH <sub>4</sub> 0-5% CO

\*Error bars are 0.5% for elemental compositions from replicate runs

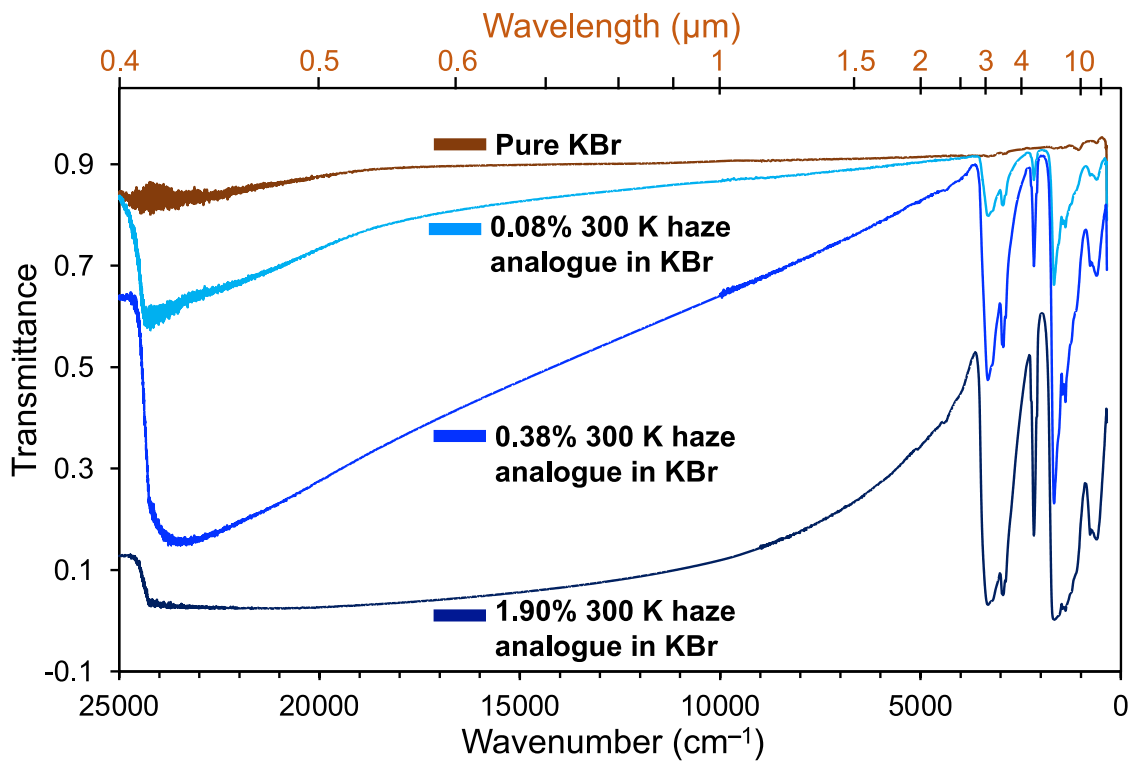
**Supplementary Table 2.** The haze parameters used in the atmospheric transmission spectra simulation for Fig.4. in the main text.

	Water-rich haze 400 K		Water-rich haze 300 K	Titan haze analogue
	Diameter/nm	Distribution/%	Same as 400 K haze	Same as 400 K haze
Particles size distribution <sup>76</sup>	31	0.00111044		
	32	0.00222089		
	33	0.00444178		
	34	0.00777311		
	35	0.01110445		
	36	0.01887756		
	37	0.03331335		
	38	0.05552224		
	39	0.09994004		
	40	0.16656673		
	41	0.33313345		
	42	0.55522242		
	43	0.82172918		
	44	1.22148933		
	45	1.71008506		
	46	2.29862083		
	47	2.97599218		
	48	3.48679681		
	49	3.99760144		
	50	4.27521265		
	51	4.41957048		
	52	4.49730162		
	53	4.51951052		
	54	4.50840607		
	55	4.48619717		
	56	4.44177938		
	57	4.37515269		
	58	4.308526		
	59	4.16416817		
	60	4.03091478		
	61	3.88655695		
	62	3.68667688		
	63	3.42239101		

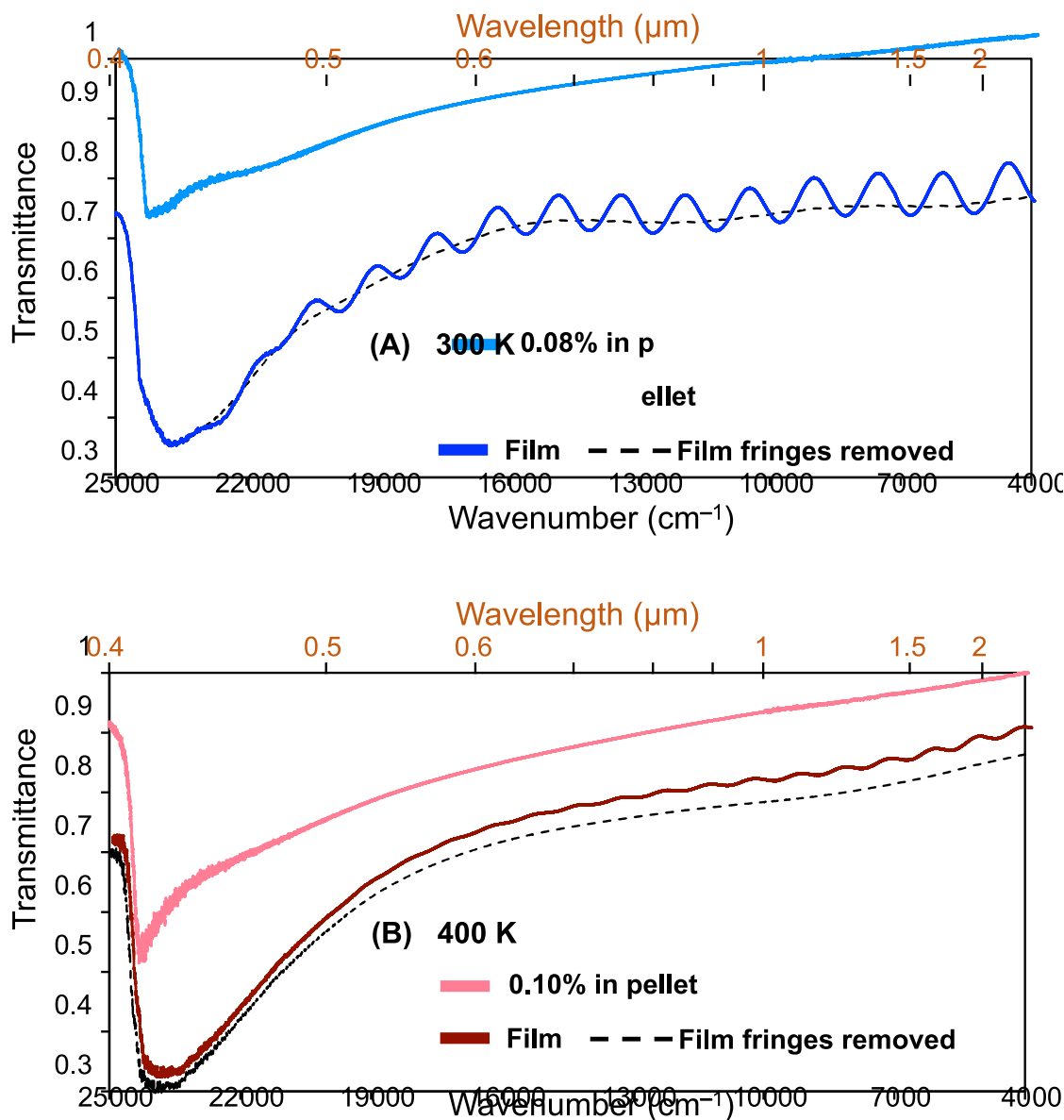
	64	3.16476781		
	65	2.81497768		
	66	2.36524752		
	67	1.99880072		
	68	1.55462278		
	69	1.27701157		
	70	0.98829591		
	71	0.85504253		
	72	0.76620694		
	73	0.6884758		
	74	0.62184911		
	75	0.58853577		
	76	0.55522242		
	77	0.52190908		
	78	0.48859573		
	79	0.47749128		
	80	0.44417794		
	81	0.42196904		
	82	0.39976014		
	83	0.37755125		
	84	0.35534235		
	85	0.322029		
	86	0.29982011		
	87	0.26650676		
	88	0.22208897		
	89	0.16656673		
	90	0.08883559		
	91	0.04441779		
	92	0.0222089		
	93	0.01110445		
	94	0.00555222		
	95	0.00111044		
Optical constants	This study		Khare et al. 1984 <sup>14</sup>	
Mass load	~25 particle/cm <sup>3</sup>			
Vertical profile	Isobaric haze layer from a pressure of 0.1 bar to 0.1 μbar			

**Supplementary Table 3.** The fringe spacings observed in the variable angle reflectance spectra of haze analogue films (Supplementary Figure 3) and the  $n_0$  values determined from Eq. 5. from 0.5-1.1  $\mu\text{m}$ .

Fringe spacing ( $\text{cm}^{-1}$ )	400 K film		300 K film	
	15 °	45 °	15 °	45 °
	961	1057	1480	1639
	966	1079	1509	1646
	972	1068	1502	1656
	965	1058	1489	1642
	976	1063	1492	1632
	972	1079	1496	1647
	977	1066		
	985	1075		
	989			
Average spacing ( $\text{cm}^{-1}$ )	973.7	1068.2	1494.7	1643.7
Standard deviation	6.2	8.6	10.1	8.1
$n_0$ value	1.6213		1.6027	
Uncertainty of $n_0$	1.3%		1.6%	

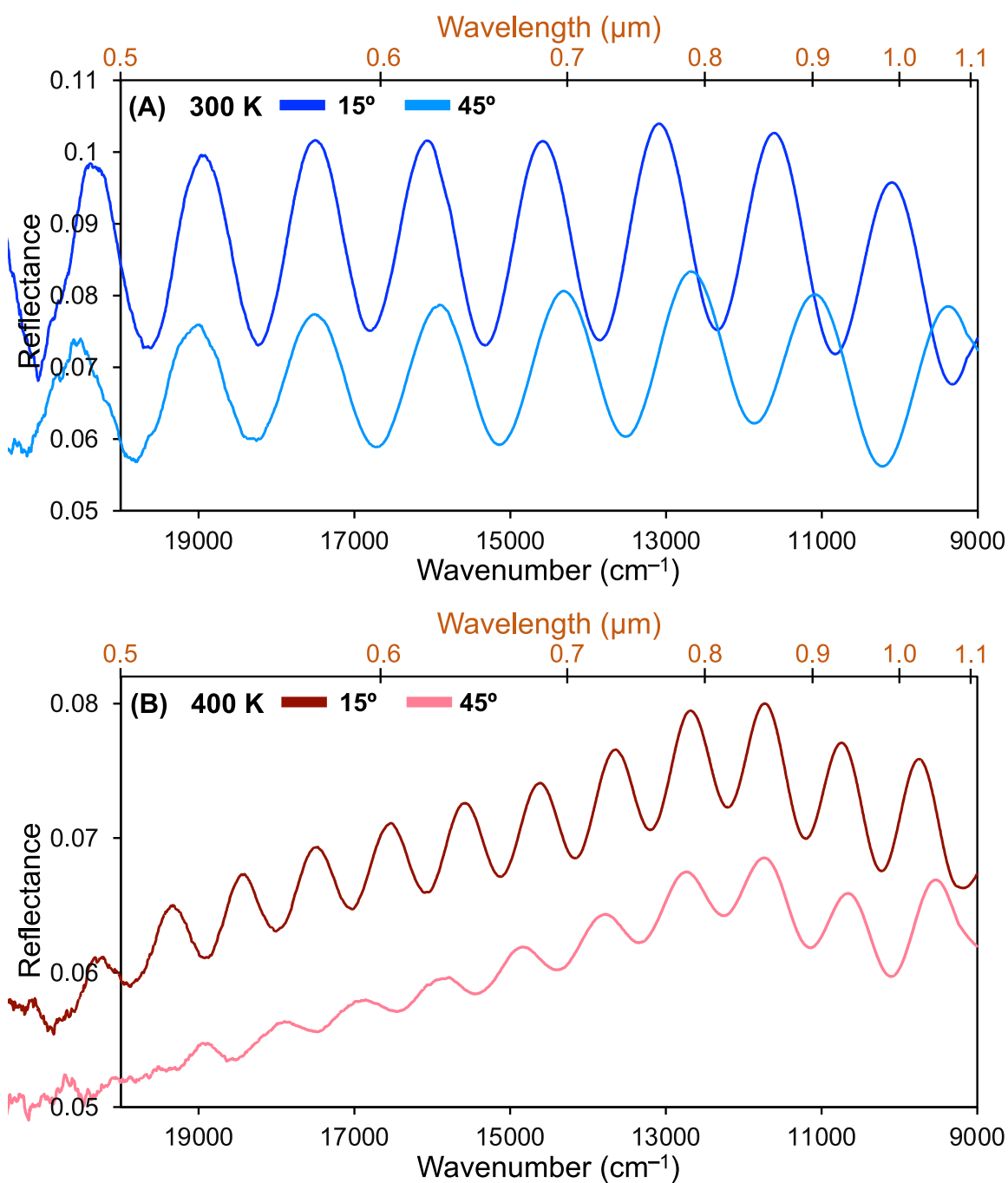


**Supplementary Figure 1.** The transmittance of pure KBr (brown) and the 300 K haze analogue in KBr with different concentrations (lighter blue: 0.08%, blue: 0.38%, darker blue: 1.9%). The spectra are referenced to the vacuum measurement without sample.

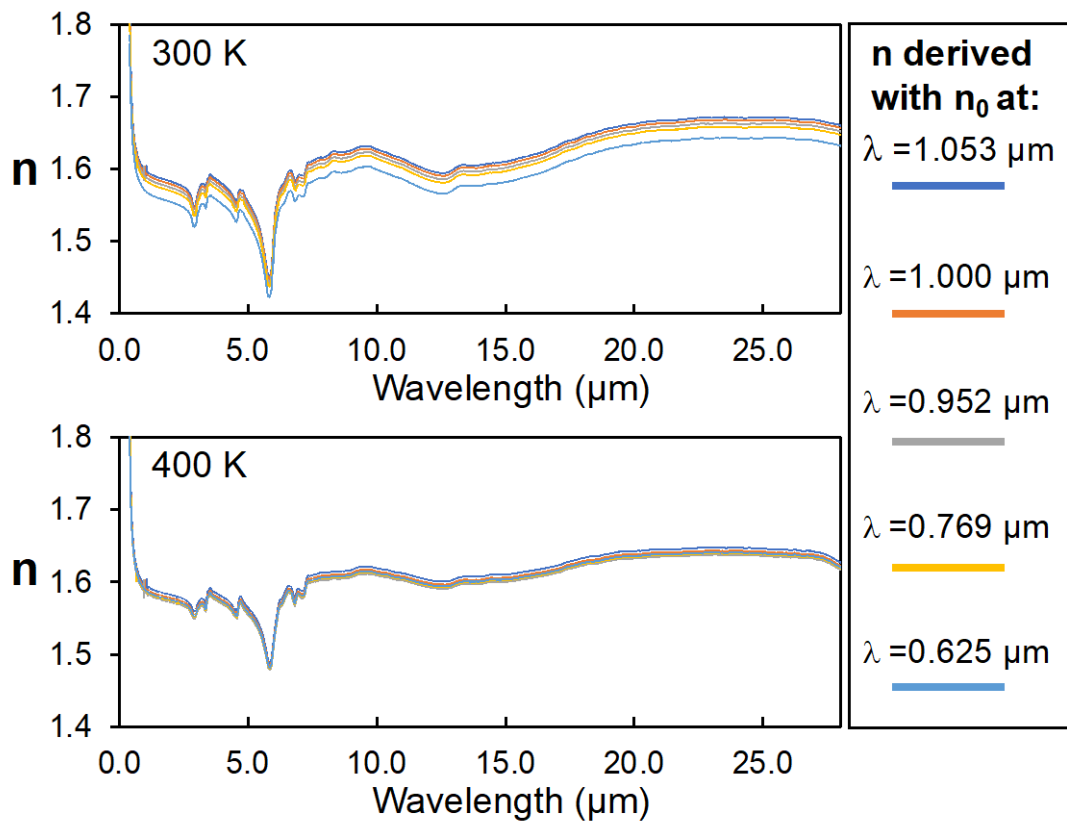


**Supplementary Figure 2.** The transmittance of the 300 K haze analogue (panel A: lighter blue-0.08% powder in KBr pellet, blue-film on quartz substrate) and 400 K haze analogue (panel B: lighter red-0.10% powder in KBr pellet, red-film on quartz substrate) from 4000 to 25000 cm<sup>-1</sup> (or from 0.4 to 2.5 μm, the quartz substrate is not transparent beyond 2.5 μm, limiting the transmittance measurements of the films in the longer wavelengths). The dashed lines are the transmittance of the films with the fringes removed. The film samples and the powder samples have similar spectral trends in this wavelength range.

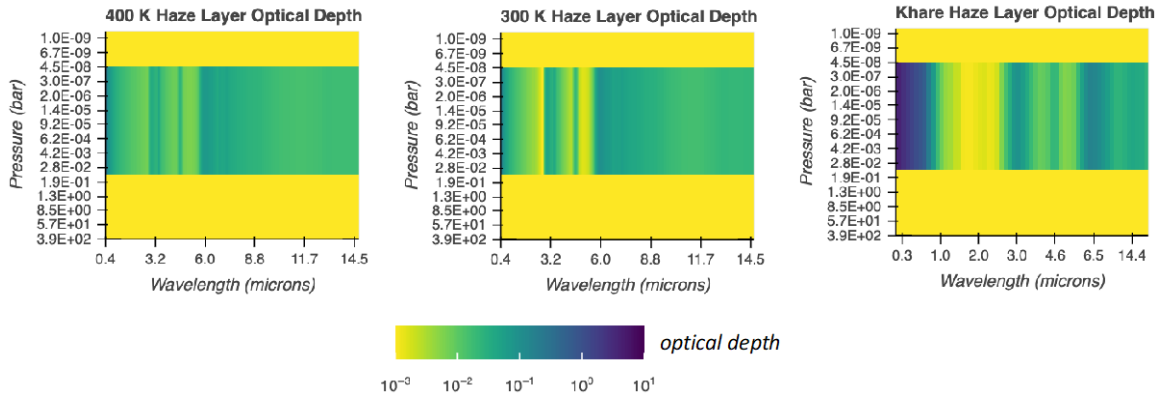




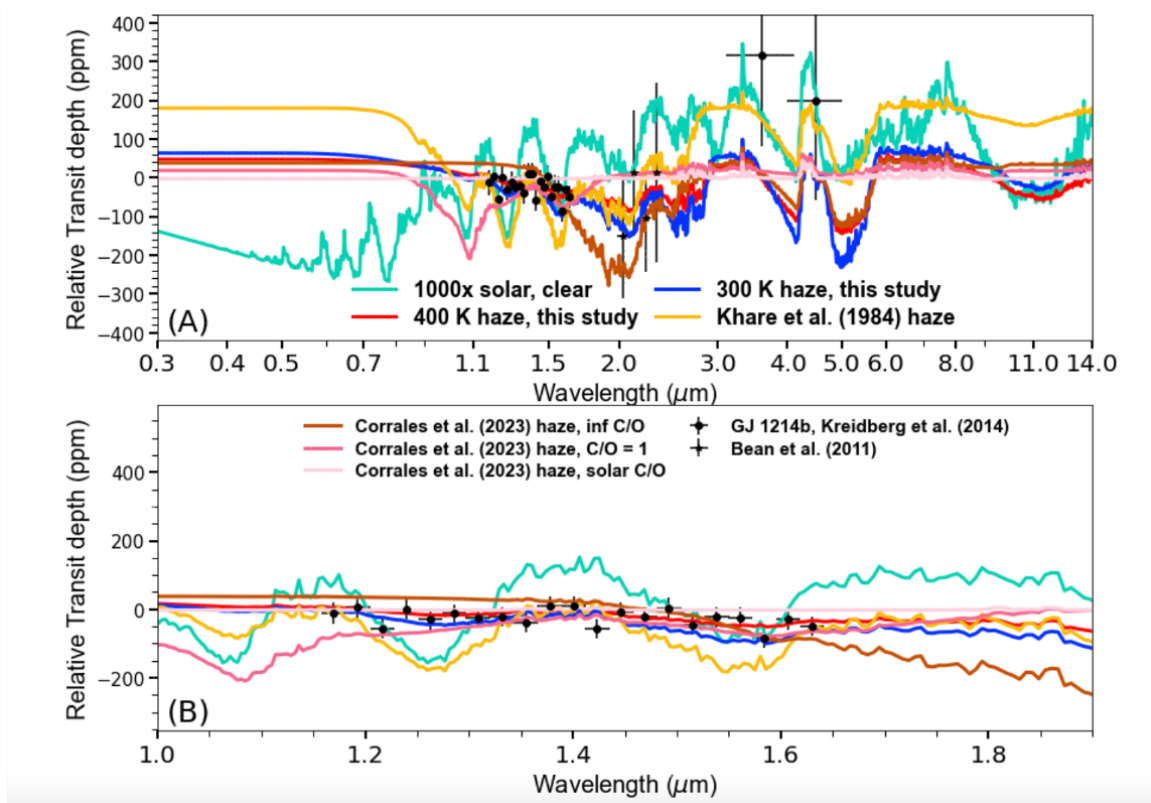
**Supplementary Figure 3.** Reflectance spectra of two exoplanet haze analogues formed in water-rich gas mixtures at 300 K (A) and 400 K (B). Using Seagull Variable Angle Reflection Accessory, we measure the reflectance of each haze analogue film at two different angles of incidence, 15° (darker shade) and 45° (lighter shade). The spectra from 20000 to 9000  $\text{cm}^{-1}$  (0.5 to 1.1  $\mu\text{m}$ ) are shown here. From the interference fringes on the reflectance spectra at two different angles, the  $n_0$  values of the samples at corresponding wavelengths can be determined using Eq. 5.



**Supplementary Figure 4.** The real refractive index ( $n$ ) for the 300 K (upper panel) and 400 K (lower panel) haze analogues derived from Eq. 6 with anchor points ( $n_0=1.6213$  for 400 K sample,  $n_0=1.6027$  for 300 K sample) at different wavelengths ( $\lambda$ ). The yielded  $n$  values for each sample are very close (the relative standard deviation is less than 2%) when different anchor points are used.



**Supplementary Figure 5.** Modeled haze slab profiles as a function of pressure and wavelength as implemented with the *Virga*-derived Mie coefficients. The color bar indicates the optical depth at each wavelength, with darker shading corresponding to higher optical depths. The haze layer extends from 0.1 bar to 0.1  $\mu$ bar with a haze particle radii distribution centered around 25 nm. Note that the Khare et al. (1984) data has wider wavelength coverage than shown, but at lower resolution than our measured optical properties.



**Supplementary Figure 6.** Model spectra of a water-rich atmosphere around a GJ 1214 b-like planet. Here we add the synthetic spectra using the optical constants reported by Corrales et al. (2023)<sup>53</sup> to show the effect of different haze optical properties. The method and settings for generating the spectra here are the same as described in 4.5. Compared to our water-rich atmospheric haze analogues and Khare Titan haze analogue, the haze analogues from Corrales et al. (2023)<sup>53</sup> more heavily mute the atmospheric spectral features in the longer wavelengths (2.5 to 14  $\mu\text{m}$ ). In the short wavelengths, the haze analogues from Corrales et al. (2023)<sup>53</sup> mute the atmospheric features at similar level as our water-rich atmospheric haze analogues. The error bars for the observed data from Kreidberg et al. (2014)<sup>1</sup> and Bean et al. (2011) correspond to  $1\sigma$  uncertainties.